Hydrated Silica Exterior Produced by Biomimetic Silicification Confers Viral Vaccine Heat-Resistance

Guangchuan Wang,[†,‡] Hong-Jiang Wang,[‡] Hangyu Zhou,[†,‡,§] Qing-Gong Nian,[‡] Zhiyong Song,[†,‡,§] Yong-Qiang Deng,[‡] Xiaoyu Wang,[†,‡,§] Shun-Ya Zhu,[‡] Xiao-Feng Li,[‡] Cheng-Feng Qin,[*,‡] and Ruikang Tang[*,†,§]

[†]Qiushi Academy for Advanced Studies, Zhejiang University, Hangzhou 310027, China, [‡]Department of Virology, State Key Laboratory of Pathogen and Biosecurity, Beijing Institute of Microbiology and Epidemiology, Beijing 100071, China, and [§]Center for Biomaterials and Biopathways, Zhejiang University, Hangzhou 310027, China

ABSTRACT Heat-lability is a key roadblock that strangles the widespread applications of many biological products. In nature, archaeal and extremophilic organisms utilize amorphous silica as a protective biomineral and exhibit considerable thermal tolerance. Here we present a bioinspired approach to generate thermostable virus by introducing an artificial hydrated silica exterior on individual virion. Similar to thermophiles, silicified viruses can survive longer at high temperature than their wild-type relatives. Virus inactivation assays showed that silica hydration exterior of the modified virus effectively prolonged infectivity of viruses by ~10-fold at room temperature, achieving a similar result as that obtained by storing native ones at 4 °C. Mechanistic studies indicate that amorphous silica nanoclusters stabilize the inner virion structure by forming a layer that restricts molecular mobility, acting as physiochemical nanoanchors. Notably, we further evaluate the potential application of this biomimetic strategy in stabilizing clinically approved vaccine, and the silicified polio vaccine that can retain 90% potency after the storage at room temperature for 35 days was generated by this biosilicification approach and validated with *in vivo* experiments. This approach not only biomimetically connects inorganic material and living virus but also provides an innovative resolution to improve the thermal stability of biological agents using nanomaterials.

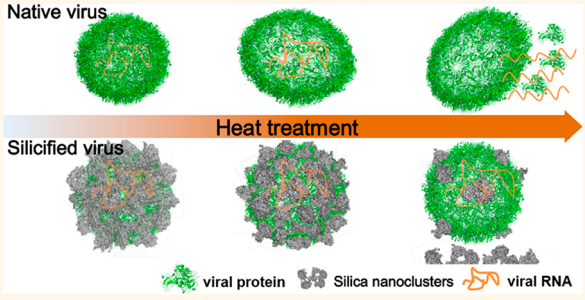

KEYWORDS: biomimetic · silicification · virus · vaccine · thermal stability · hydrated silica

Most organisms and biological products are highly heat-sensitive, a significant obstacle to their more widespread applications. For example, viruses, the smallest microbes which have thrived for billions of years on the Earth, are highly sensitive to heat. High temperatures destroy viral structures and reduce infectivity; therefore, viral vaccines and related biologicals require continuous refrigeration (cold storage) to maintain their potency.[1] Most vaccines unavoidable lose substantial potency from the time of manufacture to the point of administration. For example, about 50% of vaccine products are finally discarded due to poor thermal stability.[2] On the other hand, there are still millions of death caused by infectious diseases that are preventable with present available but underused vaccines,[3,4] because the regions most affected by the mortality and morbidity of these infectious diseases are still lack of extensive and reliable refrigeration and distribution facilities.

Therefore, developing robust vaccines less dependent on cold chain has the potential to extend vaccination program to the world's poorest communities. Currently, enhancing the thermal stability of vaccines represents an important challenge to improving global health.[5] Various natural inspired approaches have been developed to produce thermostable vaccines. With gelatin, deuterium oxide, $MgCl_2$, and nonreducing sugars as stabilizers, many stabilized vaccine formulations in liquid or dry forms are developed.[4,6−8] Through tailoring the physicochemical properties of viral capsid by reverse genetics, the thermal stability of vaccines can also be rationally engineered.[9,10] However, these methods either involve complicated treatment procedures

* Address correspondence to rtang@zju.edu.cn, qincf@bmi.ac.cn.

Received for review November 6, 2014 and accepted January 9, 2015.

Published online January 09, 2015
10.1021/nn5063276

or moderate thermal stability improvement, and novel thermal stabilization approaches should be developed.

Organisms that thrived on early Earth include many thermophilic or even hyperthermophilic species, as the living conditions then have been characterized as warmer and more acidic than current conditions due to the strong influence of hydrothermal activity.[11,12] According to fossil records, these ancient thermophiles were usually encased in silica because the concentration of silica in the Archean oceans and hydrothermal fluids was high.[11,13] Various modern organisms, ranging from hot-spring bacteria[13] to deep-sea sponges [14] and from lower unicellular diatoms[15] to higher multicellular rice plants,[16,17] retain their ability for silicification, which is used to protect themselves against environmental aggressions. Silicified phages have been identified in nature,[12] and the silicification has been suggested to be critical for their preservation and dispersal.[18,19] These phenomena indicate that biosilicification may be an evolutionarily conserved biological strategy to enhance thermal tolerance. Recently, silicification has also been used to confer cells cytoprotective coatings.[20,21] The previous studies have demonstrated that the biosilicification process in organisms is spatial and temporal controlled by using organic molecules, such as cationic polypeptides and polyamines.[22−25] Cationic amino residue-rich regions are commonly present on the capsid surface of viruses, which could be utilized as the nucleation sites for their biomimetic silicification. Inspired by these achievements, we hypothesized that biomimetic silicification would artificially confer thermal protective silica exterior on viruses.

Using human enterovirus type 71 (EV71, a typical nonenveloped picornavirus) as a model, we report a simple strategy to generate heat-tolerant viruses by introducing a hydrated silica exterior using biomimetic silicification and also provide mechanistic insight. This feasible approach can be adapted to the silicified polio vaccine, which exhibits significantly improved thermal stability in liquid form and still can be used efficiently after the storage of more than one month at room temperature. Our thermal stabilization technology relies on the good hydration ability of silica exterior, forming a confined anhydrobiotic nanoenvironment for virus in which capsid subunits are immobilized and no chemistry can occur. Our approach suggest that an advance in biomineralization creates the possibility of stabilizing living products against the denaturing effects of heat, thus eliminating their strict dependence on cold storage.

RESULTS

Silica Exterior of Virion Produced by Biomimetic Silicification. To silicify individual virions, freshly prepared silicic acid was added to a virus suspension, and the solution pH was adjusted to mild acidic conditions to initiate the rapid *in situ* virus silicification. Under transmission electron microscopy (TEM) and scanning electron microscopy (SEM), silica nanoclusters were attached on the viral surfaces, forming dispersive nanoparticles with a diameter of about 100 nm (Figure 1A,B and Supporting Information Figure S1). The inner virion core of silicified viruses was confirmed by TEM after negatively staining them with phosphotungstic acid: the 30 nm virion was surrounded by uneven inorganic exterior (Figure 1C and Supporting Information Figure S1B). The silica attachment on viral particles was also indicated by the phenomenon that >95% silicified EV71 could be separated form solution with normal speed centrifugation (16 000 g, 5 min; Supporting Information Figure S1D). Further examination of silicified virus with electron microscopy confirmed that the introduced inorganic exterior was discontinuous, which might be composed of numerous silica nanoclusters deposited around viral particles (Supporting Information Figure S1). Energy dispersive X-ray (EDX) diffraction (Figure 1D) and Raman spectroscopy (Figure 1E) revealed that the deposited silica was in a hydrated amorphous form, similar to the natural silica coating in stress-resistant organisms.[26,27]

Biological Characteristics of Silicified Virus. The introduced discontinuous silica exterior did not affect the viral infectivity profile. Silicified EV71 (Si-EV71) caused typical cytopathic effects and exhibited antigenic expression profiles that were similar to native viruses according to indirect immunofluorescence assays (IFA). Results from IFA with EV71 specific antibodies showed that the viral antigens of Si-EV71 could be efficiently expressed in host cells, similar to that of parental EV71 (Figure 2A, green); the cell nucleus is stained by DAPI (Figure 2A, blue). The silicified viruses or viral vaccines also exhibited typical viral plaque morphologies (Figure 2B and Supporting Information Figure S2A) and proliferation patterns (according to growth curves in Figure 2C and Supporting Information Figure S2B), which were similar to those of nonsilicified viruses, indicating that the biological characteristics of the native virus were retained, which was the vital for the biomedical usage of silicified virus.

Acquired Thermo-Resistance of Silicified Virus. Silicified virus exhibited enhanced heat-resistance at elevated ambient temperatures. Native EV71 exhibited a high thermal inactivation rate; *i.e.*, approximately 1 $\log_{10}$ PFU titer loss after each 4 days of storage at room temperature (25 °C) (Figure 3A). The silica hydration exterior of the modified virus effectively prolonged infectivity at room temperature (*i.e.*, approximately 1 $\log_{10}$ PFU titer loss of silicified virus after 40 days of storage), similar to that of the native virus stored at 4 °C (Figure 3A). Virus inactivation assays at higher temperatures (37 and 42 °C) also showed that silicified exterior inhibited the rate of loss of infectivity by >6- and >10-fold, respectively (Figure 3, panels B and C).

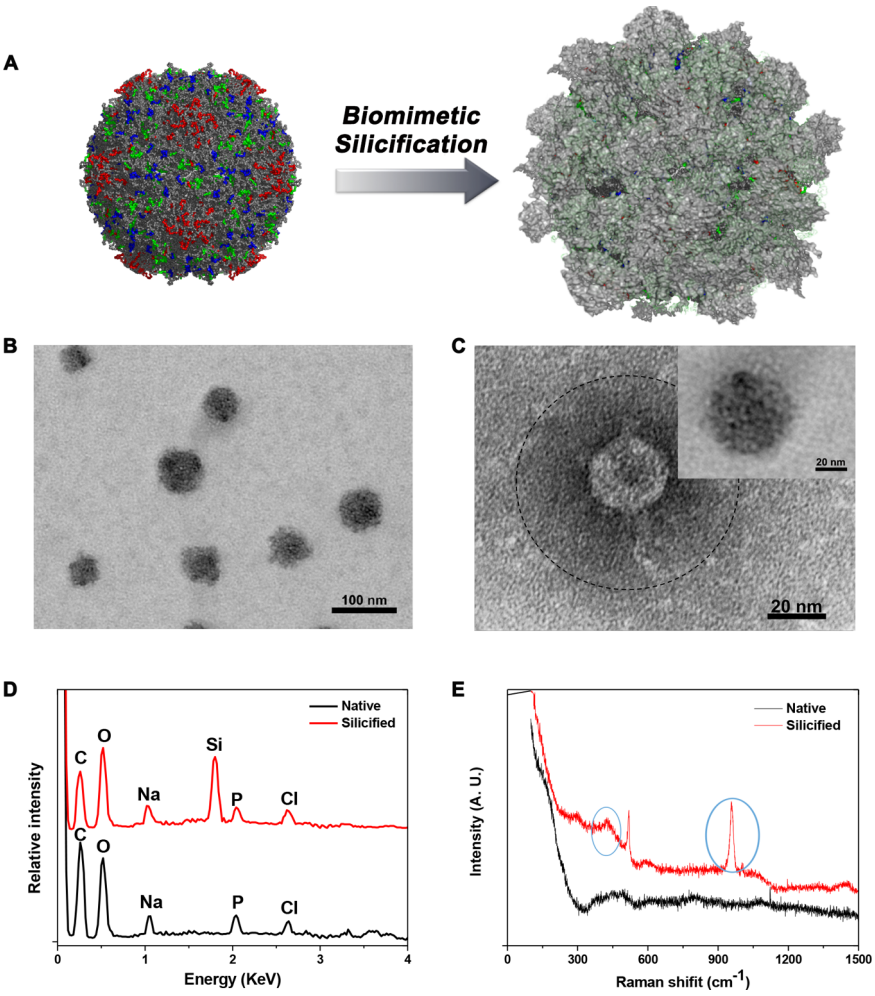

Figure 1. Electron microscopy and physicochemical characterization of silicified viruses. (A) Schematic representation of introducing exterior silica nanoclusters on virus by biomimetic silicification. The cationic amino acid-rich regions of VP1, VP2, and VP3 (red, green, and blue) act as the nucleation sites for biomimetic silicifcation of virion. (B) A TEM image of Si-EV71 that demonstrates homogeneous nanoparticles after silicification. (C) TEM images of phosphotungstic acid negatively stained Si-EV71 and the high contrast area enclosed by dotted line implied the existence of the silica exterior; the inset depicts Si-EV71 nanoparticle at high magnification. (D) EDX analyses of native and silicified EV71. (E) Raman spectra of native and silicified EV71. The peak at 966 cm^{-1} indicates that Si-EV71 contains amorphous silica.

Notably, any direct addition of silica nanoparticles or solution silicate into the virus solutions led to negligible effects on improving virus thermal stability (Supporting Information Figure S3), indicating that the *in situ* silicification rather than the addition of silica is the key to thermal stability improvement.

To further assess the thermal resistance of viruses conferred by silica exterior, we examined the difference of native and silicified viruses in thermally induced conformational changes of viral proteins and inner RNA release. The remaining EV71 viral particles adsorbed onto the host cell receptors decreased rapidly under thermal treatment; only less than 10% and approximately 0.1% viral particles retained their activity after heating at 42 °C for 24 and 72 h. In contrast, approximately 70% and 15% of the silicified EV71 viral particles retained their adsorptive ability over the same time period, representing an ~10-fold increase (Figure 3D). Typically, the dissociation of picornavirus by heat proceeds through consecutive steps, including virus swelling, conformational alteration, loosening of bonds, and RNA release.[28,29] To investigate the heat-induced dissociation of viral capsids, we studied changes of native and silicified viruses with increasing temperatures using differential scanning microcalorimetry (microDSC) and tryptophan fluorescence emission spectra (indicative of viral conformational transition). In our microDSC analysis, thermograms of native and silicified viruses both presented only one asymmetric ΔC_p peak, but the peak temperatures were approximately 65 and 78 °C, respectively (Figure 3E). This result implied that the silica hydration coating increased the temperature and energy required for conformational changes and denature of the modified viruses. Accordingly, the tryptophan fluorescence emission spectra suggested that *in situ* silicified exterior could protect the inner virus by decreasing virus-solution collisions or internal

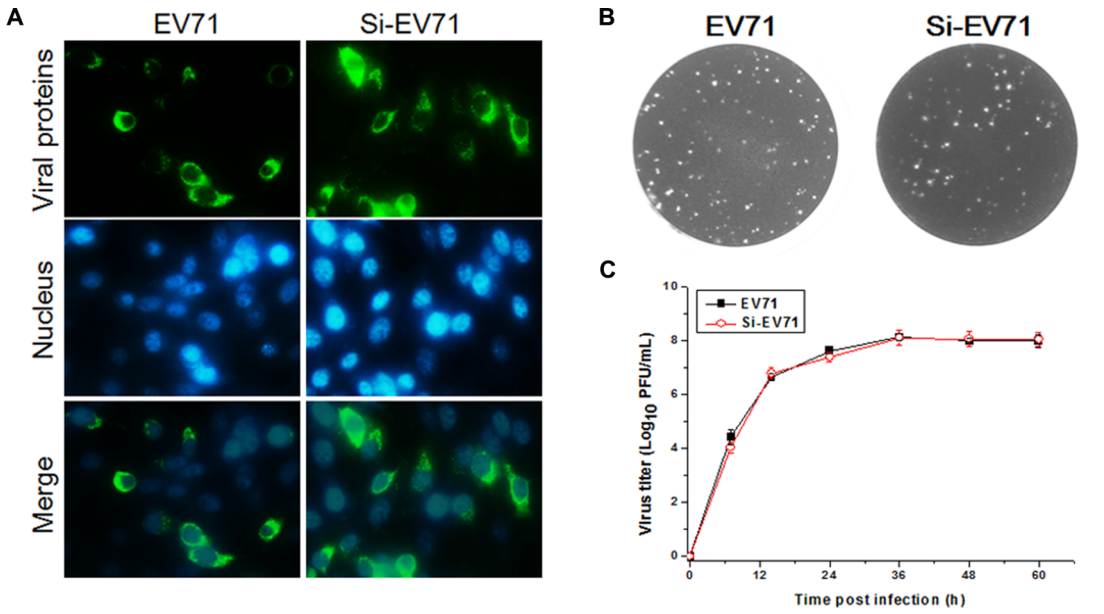

Figure 2. Biological characteristics of native EV71 and silicified EV71 viruses. (A) Indirect immunofluorescence assays (IFA) of the viruses in Vero cells using an EV71-specific antibody (green fluorescence); the cell nuclei were stained using DAPI (blue fluorescence). (B) Plaque morphology test. (C) Growth curves of EV71 and Si-EV71 in RD cells (M.O.I. = 0.1; $n \geq 3$). The error bars represent standard deviations.

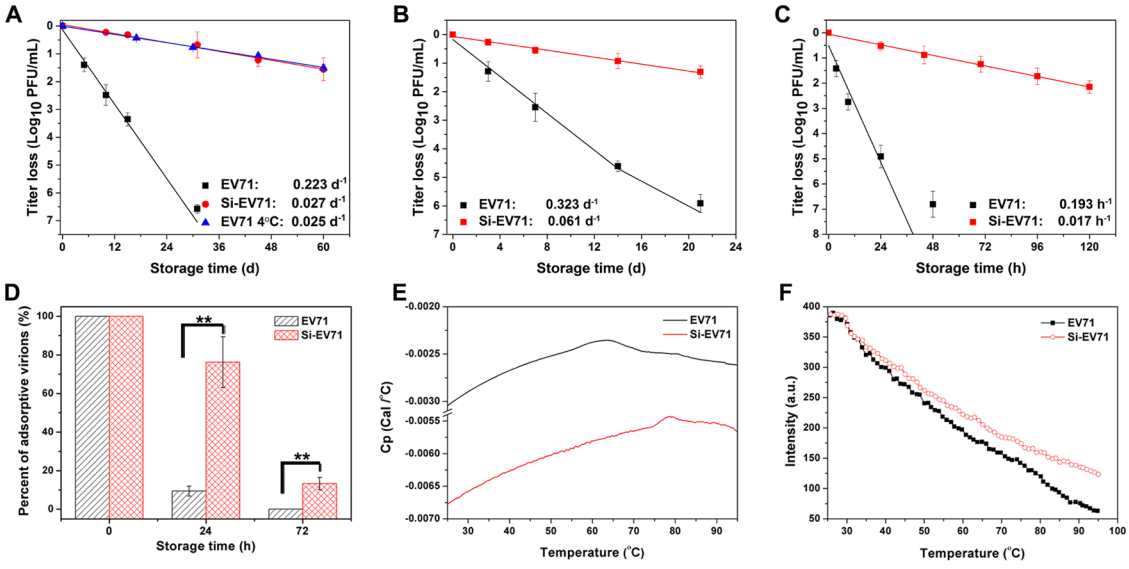

Figure 3. Acquired thermo-resistant properties of silicified viruses. (A) Thermal inactivation kinetics of EV71 and Si-EV71 at 25, (B) 37, and (C) 42 °C, with the inactivation kinetics of native EV71 at 4 °C as a reference ($n \geq 4$). The calculated average inactivation rate constants for them were shown in the corner. (D) The binding ratios of fresh or thermal treated (42 °C for 24 or 72 h) EV71/Si-EV71 on host cells ($n \geq 3$, Student's paired t test, one tailed, $^{**}P < 0.01$). (E) MicroDSC thermograms demonstrate that EV71 and Si-EV71 exhibit transitions at approximately 65 and 79 °C, respectively, indicating the thermal denature of viruses. (F) Heat-induced conformational transition of native EV71 and Si-EV71 viral particles followed by the variation in tryptophan fluorescence, and the data are plotted as normalized thermal dissociation curves. The error bars represent standard deviations.

vibrations of viral proteins (Figure 3F and Supporting Information Figure S4).

Protection Mechanism of Silica Exterior. The protection of the inner virion offered by the silica exterior and their exfoliation during vigorous thermal treatment was studied using dot-blotting assays. Under native state, viral surface proteins could be immunologically detected by EV71-specific antibodies, whereas most viral proteins of Si-EV71 could not be detected after *in situ* silicification treatment due to the formation of silica exterior (Figure 4A). However, many these proteins could be immunologically detected again after vigorous thermal treatment (Figure 4A), demonstrating the protective effect of the hydrated silica exterior and the exfoliation of silica nanoclusters under violent thermal stress. In addition, the inhibition of

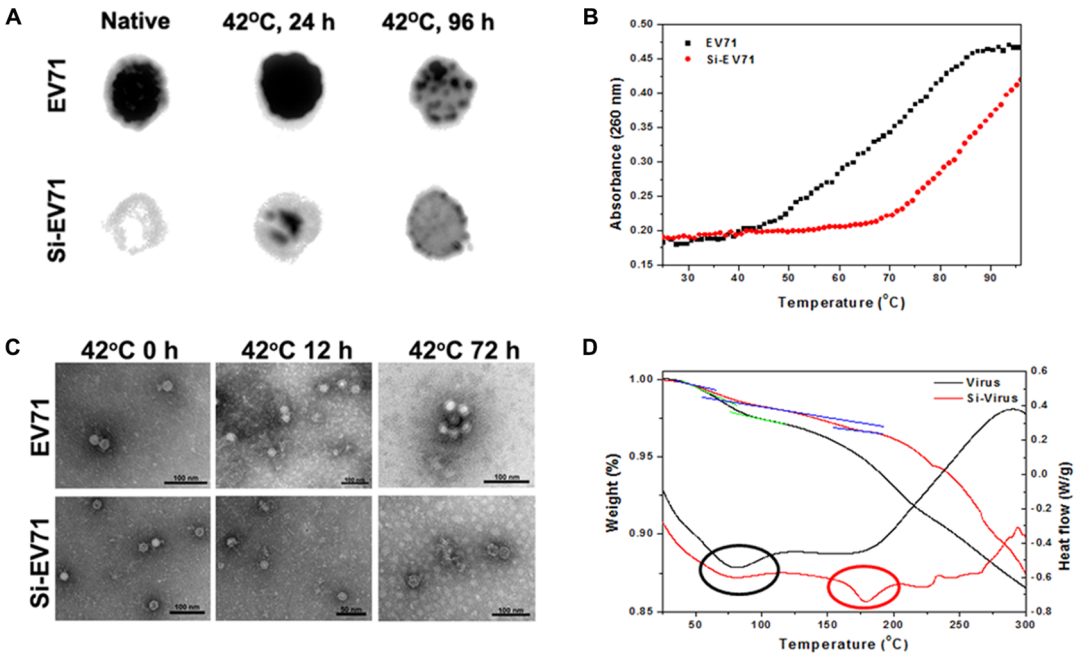

Figure 4. Mechanisms that cause the thermal stabilization of viruses based on hydrated silica anchors. (A) Dot blotting assays of native EV71 and Si-EV71, or them after thermal treatment with EV71-specific antibodies. (B) Thermally induced RNA release from native and silicified viral capsids was probed using UV absorbance at 260 nm. The results are represented as normalized thermal dissociation curves. (C) TEM images of native and silicified viruses before and after heat treatment. The results reveal that heating induces a conformational change and RNA release. (D) Combined TGA-DSC analyses of native or silicified EV71 virus powders. The results indicate the confinement of water around the silicified viruses by silica nanoclusters.

heat-induced conformational changes by the silica exterior was confirmed after examining the release of RNA. The absorbance of native viruses at 260 nm started to increase following a sigmoidal curve at 50 °C, and the midpoint of hyperchromicity T_m was approximately 70 °C. However, for silicified viruses, the absorbance began to increase at 70 °C and exhibited a T_m of approximately 85 °C (*i.e.*, approximately 15 °C higher than that of native viruses (Figure 4B)). This increase in T_m indicates that the exterior silica nanoclusters can prevent RNA release at high temperatures (Figure 4C).

The attached silica nanoclusters may prevent viral protein conformational changes due to the physiochemical confinement effects.[30] In particular, amorphous silica has been shown to confine nearby water molecules through strong hydrogen bonding.[31,32] The anchored silica nanoclusters are assumed to produce a structured hydration layer covering the exterior of virus, thereby effectively decreasing the transfer of thermal motion from the external aqueous solution to the virus interior at high temperatures. Combined thermogravimetric and differential scanning calorimetry (TGA-DSC) analyses were performed to indicate the existence of hydration layers by measuring the dependence of sample weight loss on temperature changes and related heat flow. The native and silicified samples both displayed apparent weight loss and a corresponding heat adsorption peak at 50−100 °C (Figure 4D), representing the loss of free water. Most of the water was lost from the native samples at temperatures of <100 °C, whereas the silicified viruses exhibited further specific weight losses (1.5 wt %) and heat adsorption peaks at ∼170 °C (Figure 4D), indicating the loss of confined water molecules from the silica hydration layer. This result suggests that amorphous silicified nanoclusters and nearby water molecules form an exterior hydration layer that improves the thermal stability of the encased viral particle. Taken together, these results imply that the thermal resistance conferred by silicification can be attributed to the conformational stabilization provided by the hydrated silica exterior, which might protect against thermal motion and form anchors that fix the structural conformation of interacting proteins.

Silicified Vaccine Preserve Efficacy after Long-Term Storage. We proposed that this silicification strategy inspired by nature could be developed as a general approach to stabilize many viral vaccines. With a clinically used polio vaccine, we explored the possibility of producing thermostable vaccines with this approach. Polio vaccine was biomimetically silicified under silica-rich conditions (Supporting Information Figure S5), and after modification, its thermal degradation was decreased about 6-fold (Figure 5A and Supporting Information Figure S6). The silicified polio vaccines (Si-Polio) can be stored at room temperature (25 °C) for longer than 35 days with <1 $\log_{10}$ PFU loss of potency, thereby achieving a similar result as that obtained by storing native virus at 4 °C (Figure 5A). Groups of BALB/c mice

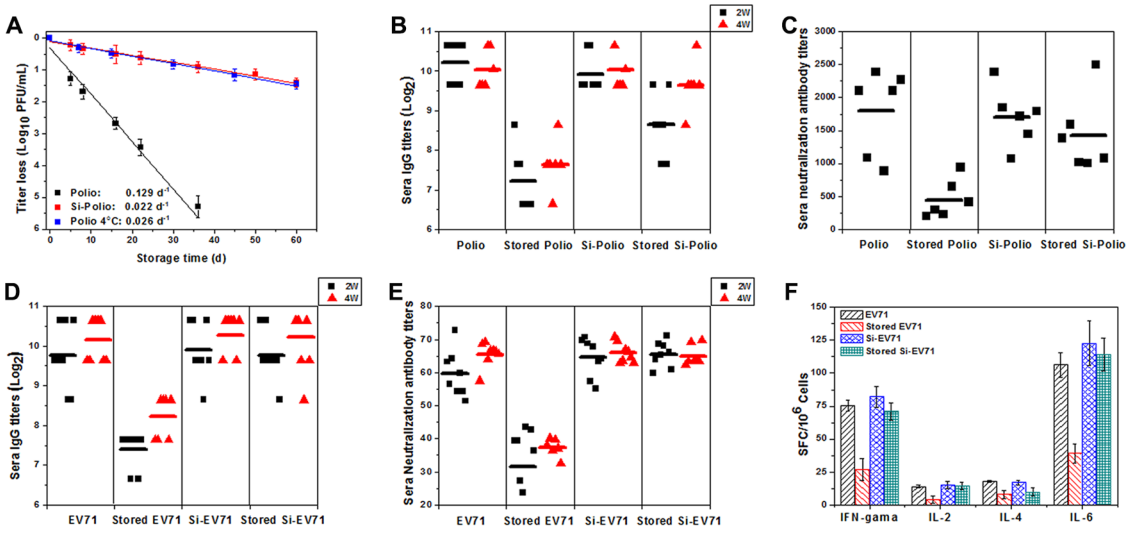

Figure 5. ***In vitro*** **and** ***in vivo*** **examinations of the use of silicification to prepare thermostable vaccines. (A) Thermal inactivation kinetics of native polio and Si-Polio at 25 °C; the stability of the polio vaccine at 4 °C is shown as a reference (*n* ≥ 4). The calculated average inactivation rate constants for them were shown in the corner. (B) The poliovirus-specific sera IgG and (C) neutralization antibody titers of mice immunized with fresh polio and Si-Polio, or with polio and Si-Polio that were stored for 4 weeks at 25 °C. Antibody titers were determined at 2 and 4 weeks postimmunization (*n* ≥ 6). (D and E) Animal experiments with fresh EV71 and Si-EV71, or with EV71 and Si-EV71 that were stored for 4 weeks at 25 °C. (D) The EV71-specific sera IgG titers, and (E) neutralization antibody titers of immunized mice at 2 and 4 weeks postimmunization (*n* ≥ 6). (F) The frequencies of EV71-specific cytokines-secreting splenocytes in immunized mice at 2 weeks postimmunization (*n* ≥ 3). The error bars represent standard deviations.**

were subcutaneously immunized to confirm the efficacy and thermal stability of the silicified vaccines. Enzyme-linked immunosorbent assays (ELISA) and standard plaque reduction neutralization tests (PRNT) demonstrated that 1 month stored Si-polio (25 °C) still effectively elicited high levels of sera IgG (Figure 5B) and neutralization antibodies (Figure 5C) in mice, similar to those induced by fresh ones. In contrast, the stored polio vaccine failed to induce a robust antibody response as expected (Figure 5B,C). Animal experiments with EV71 and Si-EV71 that had been stored at 25 °C for 1 month also confirmed that the silica hydration exterior could effectively preserve the potency of vaccines to elicit humoral immunity (Figure 5D,E). Additionally, the ability of these vaccines to elicit a cellular response was determined by examining the induced levels of cytokines, including IFN-γ, IL-2, IL-4, and IL-6, in mice splenocytes.[33,34] After 1 month of storage, Si-EV71 induced high frequencies of cytokine-secreting cells in mice splenocytes (levels were decreased by <5% in comparison to levels induced by fresh Si-EV71). In contrast, the cytokine levels induced by the stored native vaccine decreased by >50% (Figure 5F). *In vivo* examinations after storing the viruses at 42 °C provided similar results (Supporting Information Figure S7). These results demonstrate that the vaccines can be stored at ambient temperature after silicification, providing an efficient method to distribute vaccines without reliable cold storage. Notably, silica/silicate is considered "Generally Recognized as Safe" by the U.S. Food and Drug Administration, and the amount of silica used in vaccine injection (<1 mg) is negligible in comparison with the reported toxic dose (~500 mg/kg).[35]

DISCUSSION

In this study, hydrated silica nanoclusters are artificially fabricated onto individual virus particles to generate thermophile-mimicking virus. Together with the mechanistic analysis, we suggest that biosilicification represents a natural evolved self-protection strategy of organisms, and this strategy can be mimicked to produce thermal protective exterior for heat-liable biological products. By adjusting solution pH, the cationic amino residue-rich regions of capsid surface of EV71 and poliovirus type II (Supporting Information Figure S8) were utilized as nucleation sites to template the nonhomogeneous deposition of silica nanoclusters around virion. Finally, we successfully fabricated a silica exterior on virus under near-physiological conditions by taking advantage of these residues as anchoring sites for silica nanoclusters and concisely tuning the concentration of silicic acid and reaction pH in virus solution.

Notably, the discontinuous nature of silica exterior is of high importance for the preservation of virus infectivity and vaccines potency. Our results revealed that the introduction of integrated silica shell on virus at weak alkaline condition (*e.g.*, pH 8.0) would result in almost complete loss of infectivity, as the disassociation of viral capsid is totally prohibited by the mineral. With the introduction of this kind of discontinuous silica coating with virion nonhomogeneous silicification at weak acidic condition, we could take advantage

of the thermal protective role of hydrated silica without severely impairing the inherent biological property of viruses. This exterior silica nanoclusters are rather stable under extracellular condition. However, the silicified viruses could undergo similar uncoating after the internalization by cells, RNA releasing and replication process as the native ones (Figure 2 and Supporting Information Figure S2). Therefore, hydrated silica exterior does not hinder the infectivity of virus and the biosilicified ones share similar replication and growth pattern with native ones.

Previously, we have proposed and demonstrated the use of a calcium-based biomineralization strategy to develop thermostable vaccines.[36] Strikingly, silicification treatment prolongs the storage period of vaccines at room temperature by approximately 10-fold. This increase compares with the only 3-fold improvement by calcification, indicating the advantage of silicification over calcification approach for providing protection against thermal stress. This advantage might be due to the better hydration ability of silica than calcium biominerals such as calcium phosphates and calcium carnbonates. The other attempts have demonstrated that vaccines can also be stabilized by the addition of trehalose, $MgCl_2$, and D_2O,[8,37] because the water surrounding vaccines is either confined by the formation of hydrogen bonds with these stabilizing agents or is directly lost. Thus, factors promoting protein degradation, such as chemical reactions and bond exchanges, are reduced.[7,38] Compared with these other stabilizing agents, silica also exhibits a favorable H_2O confinement effect but may be a superior agent due to its controllable polymerization property. With these properties, kinds of silica formulations have been developed to improve the performance of organism in harsh environments, as confined aqueous microenvironments can be formed around biologicals to decrease their degradability.[39,40] In the present study, a discontinuous but protective silica hydration exterior rather than a simple shell structure is fabricated for individual virus at biocompatible conditions. By forming hydrogen bonds with nearby water molecules, these discontinuous silica nanoclusters form a protective hydration exterior, which can maintain rather constant inner nanoenvironment for viruses to protect them against destructive factors such as molecular mobility, pH and ionic strength shift.

With the use of clinically approved polio vaccine as a model, we further demonstrated the potential applications of this strategy to produce thermostable vaccines. Both *in vitro* and *in vivo* experiments demonstrated that silicified vaccine still could be efficiently used to elicit humoral and cellular immune response in mice after 1 month of room temperature storage. Currently, the high death toll of vaccine-preventable infectious disease still represents the majority of deaths in developing regions lacking extensive, reliable refrigeration infrastructure due to the poor thermal stability of vaccines.[1,3] The current achievement also means that we may realize the vaccine of "at pocket for 1 month" in liquid formulation, without freeze-dry and reconstitution prior to injection. Besides, such fast, cheap approach can easily be adapted to any other vaccines. For example, virus like particle vaccines and other biological products can also be modified with a silica hydration exterior to improve their thermal stability. In general, the analogous thermal improvement by biomimetic silicification can be utilized in more vaccines, and this strategy may hold significant promise for providing a feasible path to large-scale production of thermostable vaccine.

CONCLUSIONS

We have demonstrated that an artificial silica hydration exterior could be introduced on individual virus by biomimetic silicification and this exterior can confer virus heat-desiccation resistance by creating rather constant nanoenvironment. This strategy can be developed as a general approach to prepare thermostable vaccines, thus efficiently decreasing the cost of vaccine delivery. This study is based on the concept that an amorphous silica hydration exterior may be evolved as a protective strategy by living organisms against thermal stress, and this concept can be biomimetically followed to improve the stability of biological products with nanomaterials.

METHODS

Cells and Viruses. Human rhabdomyosarcoma (RD) cells, baby hamster kidney (BHK) cells, and African green monkey kidney (Vero) cells were obtained from the American Type Culture Collection (ATCC) and were cultured in Dulbecco's Modified Eagle Medium (DMEM) supplemented with 10% fetal bovine serum (FBS) at 37 °C and 5% CO_2. Human EV71 strain A12 was isolated from hand, foot, and mouth disease patients, and *in vitro* and *in vivo* characterization demonstrated that the A12 strain was nonvirulent in suckling mice with ideal attenuated characteristics.[41] Human poliovirus Sabin type II OPV strain (P712 Ch 2ab) was kindly provided by the Chinese National Institute for Food and Drug Control. All virus stocks were prepared and titrated in RD cells; the stocks were stored at −70 °C until use.

Biosilicification Treatments. Silicic acid (30 mM) was prepared fresh before use as follows: 5.3 μL of sodium silicate (Sigma) was diluted in 1 mL of PBS (pH 7.4); 20 μL of 1.25 M HCl was then added to adjust the solution to pH 7.5−8.0. To obtain *in situ* silicified viruses, 30 mM silicic acid in PBS and virus solution (10^8−10^9 PFU/mL) were mixed at a ratio of 1:9 and stirred for 5 min. The pH was adjusted to 5.5−6.5 with HCl to initiate silicification, reacting for 15−30 min. Silicification was terminated by adjusting the pH to 7.0.

Electron Microscopy. Solutions containing viruses were dropped onto carbon-coated copper TEM grids (400 meshes,

Agar Scientific). The samples were dried at room temperature before observation. After negative staining with phosphotungstic acid, TEM observations were performed using a JEM-1200EX instrument (JEOL, Japan). SEM and EDX analyses were conducted using an S-4800 instrument (HITACHI, Japan).

Plaque Assays. RD cells at 90% confluence in 12-well plates were infected with 333 μL of serially diluted virus particles. After allowing adsorption for 1 h, the infected cells were washed and then incubated for 3 days in DMEM supplemented with 2% FBS and 1% low melting point agarose. The infected cells were fixed with 4% formaldehyde and stained using a crystal violet solution (1% crystal violet, 0.85% NaCl, and 2% formaldehyde).

Thermal Stability Tests. Native EV71, Si-EV71, Polio, and Si-Polio were incubated at 4, 25, 37, and 42 °C. The samples were collected periodically, and infectivities were determined using plaque assays as previously described.[42] The remaining infectivity percentages are represented on a logarithmic scale as a function of incubation time; the data represent mean ± standard deviations.

Viral RNA Release-Temperature Curves. The changes in the UV absorbance of native and silicified EV71 virus solutions at 260 nm were measured using a Varian Cary 300 UV−vis spectrophotometer (Varian) equipped with a computer-operated Peltier temperature control unit. The cell-block was electrically heated from 25 to 95 °C at a constant rate of 2.5 °C/min, and changes in the UV absorbance at 260 nm of suspensions of native and silicified EV71 virus in DMEM solutions were measured.

Dot Blot Assays. For immunological detection of virus coat proteins, 10^6 PFU each of native EV71 and Si-EV71 viruses and of the same viruses after heat treatment were spotted onto methane-activated PVDF membranes (Millipore); after the membranes were air-dried at room temperature, nonspecific binding sites were blocked using 2% bovine serum albumin (BSA) in phosphate-buffered saline (PBS). Then, the membranes were incubated with EV71-specific polyclonal antibodies, followed by a horseradish peroxidase (HRP)-conjugated horse anti-mouse antibody. Both antibodies were diluted in blocking solution (0.05% BSA).

Indirect Immunofluorescence Assays (IFA). RD cells at 90%−100% confluence were infected with EV71 or Si-EV71 at the desired multiplicity of infection (M.O.I.). The infected cells were fixed at 12−24 h postinfection with precooled acetone at −20 °C for 30 min. The infected cells were washed with PBS and then incubated with polyclonal antibodies against EV71 for 1 h; the cells were then washed three times with PBS and incubated with Alexa Fluor 488-conjugated goat anti-mouse IgG secondary antibody for 45 min. Fluorescence was detected after PBS washing. DAPI was then added, and the cells were incubated at room temperature for 5 min to stain the nuclei.

Growth Curves. Viral growth curves in RD cells were determined by seeding native EV71, Si-EV71, poliovirus, and Si-Polio in RD cells at 90%−100% confluence in 24-well plates at the desired M.O.I. The supernatants were collected at intervals, and their viral titers were examined using plaque assays.

One-Step Quantitative Real-Time RT-PCR (qRT-PCR). RNA of samples was extracted with RNA Purelink RNA mini kit (Ambion), and one-step quantitative real-time RT-PCR was used to quantify the amount of viral RNA by using One Step PrimeScript RT-PCR Kit (Takara) with EV71 specific forward premiers (Fwd, 5′-GGCCATTTATGTGGGTAACTTTAGA-3′; Rev, 5′-CGGGCAATCGTGTCACAAC-3′) and probe (5′ FAM-AAGACAGCTCTCGCGACTTGCTCGTG-BQH1 3′). Absolute quantification of RNA was calculated according to the standard curve, which was generated by serially diluting a RNA solution of determined titer in RNase-free water.

Tryptophan Fluorescence Intensity and Polarization. To monitor conformational changes, thermal denaturation experiments were conducted using a Varian Cary Eclipse luminescence spectrophotometer (Varian) equipped with a computer-operated Peltier temperature control unit. Native and silicified EV71 viral solutions of the desired concentrations placed in a 2 mm path length (2 × 10 mm) cell were irradiated with UV light using an excitation wavelength of 295 nm. The excitation and emission slit widths were both 5 nm, and emission spectra were scanned from 310 to 400 nm. In thermal denaturation experiments, virus solutions were continuously heated from 25 to 100 °C at a rate of 60 °C/h, and the intrinsic tryptophan fluorescence at 350 nm was recorded and fitted to a sigmoid curve.

Differential Scanning Microcalorimetry (microDSC). Virus samples were concentrated and purified by ultrafiltration using an Amicon Ultra-15 filter device (30K NMWL). Native and silicified EV71 virus samples were prepared in DMEM, and measurements were performed using a Microcal MCS instrument (MicroCal). Experiments were performed under identical conditions, including obtaining thermal equilibrium at 10 °C for 30 min before increasing the heat, scanning temperature of up to 100 °C, and a scanning rate of 0.5 °C/min. The heat capacity change with respect to temperature was obtained based on DSC thermograms of the virions.

Mouse Experiments. Mice experiments were approved and performed in strict accordance with the guidelines of the Animal Experiment Committee of Beijing Institute of Microbiology and Epidemiology (China). BALB/c mice were subcutaneously immunized with fresh or stored EV71, Si-EV71, poliovirus, and Si-Polio. The initial viral titers of all samples were same before storage (200 μL, 5 × 10^7 PFU/mL). Mice sera were collected at 2 and 4 weeks postinjection, and the serum IgG and neutralization antibody titers were detected using ELISA and a microneutralization assay, respectively.

Microneutralization Tests. Mouse serum was serially diluted (2-fold each time) in DMEM, starting at 1:8. Virus suspensions (200 μL at 100 PFU) were mixed with 200 μL of diluted sera, and the mixtures were incubated at 37 °C for 1 h. The mixtures were then added to 90% confluent RD cells and incubated for 3 days. The appropriate serum, viruses, and cell controls were included in the tests. End point titers were calculated according to the Karber method, as previously described.[43]

Enzyme-Linked Immunosorbent Assays (ELISAs). EV71/poliovirus specific serum IgG antibodies were detected using indirect ELISAs in 96-well flat-bottomed plates (Costar) coated with EV71/poliovirus, which was diluted 1:100 in 0.1 M carbonate/bicarbonate buffer (pH 9.6). The plates were coated overnight at 4 °C. After a blocking step with 2% BSA in PBST, the plates were incubated with serially diluted sera in duplicate wells for 1 h at 37 °C. Peroxidase-conjugated horse anti-mouse IgG diluted in PBST (1:5000) was then added, and the plates were incubated at 37 °C for 45 min. After this time, TMB substrate was added. The plates were washed with PBST (pH 7.2) three times after each reaction. The absorbance of the plates was determined at 492 nm and corrected for background using PBS as control group sera.

ELISPOT Assays. IFN-γ, IL-2, IL-4, and IL-6 ELISPOT mouse kits (BD Biosciences) were used according to the manufacturer's instructions. Briefly, 96-well filtration plates were coated overnight at 4 °C with capture monoclonal antibody; the plates were then washed and blocked with RPMI-1640 medium containing 1% L-glutamine and 10% FBS for 2 h at room temperature. Splenocytes in RPMI-1640 (5 × 10^5 cells/well) were then added, and EV71 was subsequently added as the stimulation antigen; the plates were cultured for approximately 20 h at 37 °C and 5% CO_2. After washing steps once with water and three times with PBST, the plates were incubated with biotinylated detection antibody at room temperature for 2 h. Then, plates were incubated with HRP-conjugated streptavidin at room temperature for 1 h after washing three times with PBST. Spots were revealed using an AEC substrate reagent kit (BD Bioscience) at room temperature and counted using an Immunospot Reader (Cellular Technology).

Statistical Analyses. The statistical significance of antibody titer differences among different groups was analyzed using Student's *t*-test as implemented in SPSS software. The results with error bars are expressed as means ± standard deviations.

Conflict of Interest: The authors declare no competing financial interest.

Supporting Information Available: Figure S1, electron microscopy characterizations of silicified EV71 viruses; Figure S2, biological comparisons between native polio and silicified polio (Si-polio) vaccines; Figure S3, thermal-inactivation kinetics of native viruses and their mixtures with silica at room

temperature (25 °C); Figure S4, thermally induced conformational transition of native EV71 and Si-EV71 capsids, as probed by intrinsic tryptophan fluorescence; Figure S5, electron microscopy characterizations of silicified polio vaccines; Figure S6, thermal stability of native and silicified polio vaccines at 37 and 42 °C; Figure S7, *in vivo* examination of the vaccine potentials of Si-EV71 and native EV71 before and after thermal treatment at 42 °C for 4 days; Figure S8, schematic diagram illustrating that regions rich in cationic amino acids are abundant. This material is available free of charge *via* the Internet at http://pubs.acs.org.

Acknowledgment. We thank Prof. S. Wang (Institute of Chemistry, CAS), Prof. R. Chen (Institute Pasteur of Shanghai, CAS) and Prof. L. Wang (Huazhong Agricultural University) for their assistance with characterizing the samples and with discussions. G.W., R.T. and C.-F.Q. conceived the concept, designed the research studies and wrote the paper; G.W., H.-J. W, H.Z., Q.-G.N., Z.S. X.W. and S.-Y.Z. performed the research; G.W., Y.-Q.D., X.-F.L., R.T., and C.-F.Q., analyzed the data. Research was funded by National Natural Science Foundation of China (91127003 and 31400785), the Beijing Natural Science Foundation (7122129), and the Fundamental Research Funds for the Central Universities (ZJU President Project).

REFERENCES AND NOTES

1. Chen, X.; Fernando, G. J.; Crichton, M. L.; Flaim, C.; Yukiko, S. R.; Fairmaid, E. J.; Corbett, H. J.; Primiero, C. A.; Ansaldo, A. B.; Frazer, I. H.; *et al.* Improving the Reach of Vaccines to Low-Resource Regions, with a Needle-Free Vaccine Delivery Device and Long-Term Thermostabilization. *J. Controlled Release* **2011**, *152*, 349–355.
2. Schlehuber, L. D.; McFadyen, I. J.; Shu, Y.; Carignan, J.; Duprex, W. P.; Forsyth, W. R.; Ho, J. H.; Kitsos, C. M.; Lee, G. Y.; Levinson, D. A.; *et al.* Towards Ambient Temperature-Stable Vaccines: The Identification of Thermally Stabilizing Liquid Formulations for Measles Virus Using an Innovative High-Throughput Infectivity Assay. *Vaccine* **2011**, *29*, 5031–5039.
3. Clemens, J.; Holmgren, J.; Kaufmann, S. H.; Mantovani, A. Ten Years of the Global Alliance for Vaccines and Immunization: Challenges and Progress. *Nat. Immunol.* **2010**, *11*, 1069–1072.
4. Brandau, D. T.; Jones, L. S.; Wiethoff, C. M.; Rexroad, J.; Middaugh, C. R. Thermal Stability of Vaccines. *J. Pharm. Sci.* **2003**, *92*, 218–231.
5. Varmus, H.; Klausner, R.; Zerhouni, E.; Acharya, T.; Daar, A.; Singer, P. Public Health: Grand Challenges in Global Health. *Science* **2003**, *302*, 398.
6. Zhang, J.; Pritchard, E.; Hu, X.; Valentin, T.; Panilaitis, B.; Omenetto, F. G.; Kaplan, D. L. Stabilization of Vaccines and Antibiotics in Silk and Eliminating the Cold Chain. *Proc. Natl. Acad. Sci. U.S.A.* **2012**, *109*, 11981–11986.
7. Alcock, R.; Cottingham, M. G.; Rollier, C. S.; Furze, J.; De Costa, S. D.; Hanlon, M.; Spencer, A. J.; Honeycutt, J. D.; Wyllie, D. H.; Gilbert, S. C.; *et al.* Long-Term Thermostabilization of Live Poxviral and Adenoviral Vaccine Vectors at Supraphysiological Temperatures in Carbohydrate Glass. *Sci. Transl. Med.* **2010**, *2*, 19ra12.
8. Adebayo, A. A.; Sim-Brandenburg, J. W.; Emmel, H.; Olaleye, D. O.; Niedrig, M. Stability of 17d Yellow Fever Virus Vaccine Using Different Stabilizers. *Biologicals* **1998**, *26*, 309–316.
9. Reguera, J.; Carreira, A.; Riolobos, L.; Almendral, J. M.; Mateu, M. G. Role of Interfacial Amino Acid Residues in Assembly, Stability, and Conformation of a Spherical Virus Capsid. *Proc. Natl. Acad. Sci. U.S.A.* **2004**, *101*, 2724–2729.
10. Mateo, R.; Luna, E.; Rincon, V.; Mateu, M. G. Engineering Viable Foot-and-Mouth Disease Viruses with Increased Thermostability as a Step in the Development of Improved Vaccines. *J. Virol.* **2008**, *82*, 12232–12240.
11. Orange, F.; Westall, F.; Disnar, J. R.; Prieur, D.; Bienvenu, N.; Le Romancer, M.; Defarge, C. Experimental Silicification of the Extremophilic Archaea Pyrococcus abyssi and Methanocaldococcus jannaschii: Applications in the Search for Evidence of Life in Early Earth and Extraterrestrial Rocks. *Geobiology* **2009**, *7*, 403–418.
12. Peng, X.; Xu, H.; Jones, B.; Chen, S.; Zhou, H. Silicified Virus-like Nanoparticles in an Extreme Thermal Environment: Implications for the Preservation of Viruses in the Geological Record. *Geobiology* **2013**, *11*, 511–526.
13. Walker, J. J.; Spear, J. R.; Pace, N. R. Geobiology of a Microbial Endolithic Community in the Yellowstone Geothermal Environment. *Nature* **2005**, *434*, 1011–1014.
14. Sundar, V. C.; Yablon, A. D.; Grazul, J. L.; Ilan, M.; Aizenberg, J. Fibre-Optical Features of a Glass Sponge. *Nature* **2003**, *424*, 899–900.
15. Hamm, C. E.; Merkel, R.; Springer, O.; Jurkojc, P.; Maier, C.; Prechtel, K.; Smetacek, V. Architecture and Material Properties of Diatom Shells Provide Effective Mechanical Protection. *Nature* **2003**, *421*, 841–843.
16. Neethirajan, S.; Gordon, R.; Wang, L. J. Potential of Silica Bodies (Phytoliths) for Nanotechnology. *Trends Biotechnol.* **2009**, *27*, 461–467.
17. Wang, L. J.; Nie, Q.; Li, M.; Zhang, F. S.; Zhuang, J. Q.; Yang, W. S.; Li, T. J.; Wang, Y. H. Biosilicified Structures for Cooling Plant Leaves: A Mechanism of Highly Efficient Midinfrared Thermal Emission. *Appl. Phys. Lett.* **2005**, *87*, 194105.
18. Laidler, J. R.; Stedman, K. M. Virus Silicification under Simulated Hot Spring Conditions. *Astrobiology* **2010**, *10*, 569–576.
19. Laidler, J. R.; Shugart, J. A.; Cady, S. L.; Bahjat, K. S.; Stedman, K. M. Reversible Inactivation and Desiccation Tolerance of Silicified Viruses. *J. Virol.* **2013**, *87*, 13927–13929.
20. Lee, J.; Choi, J.; Park, J. H.; Kim, M. H.; Hong, D.; Cho, H.; Yang, S. H.; Choi, I. S. Cytoprotective Silica Coating of Individual Mammalian Cells through Bioinspired Silicification. *Angew. Chem., Int. Ed.* **2014**, *53*, 8056–8059.
21. Wang, G.; Wang, L.; Liu, P.; Yan, Y.; Xu, X.; Tang, R. Extracellular Silica Nanocoat Confers Thermotolerance on Individual Cells: A Case Study of Material-Based Functionalization of Living Cells. *ChemBioChem* **2010**, *11*, 2368–2373.
22. Belton, D. J.; Patwardhan, S. V.; Annenkov, V. V.; Danilovtseva, E. N.; Perry, C. C. From Biosilicification to Tailored Materials: Optimizing Hydrophobic Domains and Resistance to Protonation of Polyamines. *Proc. Natl. Acad. Sci. U.S.A.* **2008**, *105*, 5963–5968.
23. Kroger, N.; Deutzmann, R.; Sumper, M. Polycationic Peptides from Diatom Biosilica That Direct Silica Nanosphere Formation. *Science* **1999**, *286*, 1129–1132.
24. Kroger, N.; Deutzmann, R.; Bergsdorf, C.; Sumper, M. Species-Specific Polyamines from Diatoms Control Silica Morphology. *Proc. Natl. Acad. Sci. U.S.A.* **2000**, *97*, 14133–14138.
25. Hildebrand, M. Diatoms, Biomineralization Processes, and Genomics. *Chem. Rev.* **2008**, *108*, 4855–4874.
26. Street-Perrott, F. A.; Barker, P. A. Biogenic Silica: A Neglected Component of the Coupled Global Continental Biogeochemical Cycles of Carbon and Silicon. *Earth Surf. Processes Landforms* **2008**, *33*, 1436–1457.
27. Ma, J. F.; Yamaji, N. Silicon Uptake and Accumulation in Higher Plants. *Trends Plant Sci.* **2006**, *11*, 392–397.
28. Chen, C.-H.; Wu, R.; Roth, L. G.; Guillot, S.; Crainic, R. Elucidating Mechanisms of Thermostabilization of Poliovirus by D2o and Mgcl2. *Arch. Biochem. Biophys.* **1997**, *342*, 108–116.
29. Dimmiock, N. J. Differences between the Thermal Inactivation of Picornaviruses at "High" and "Low" Temperatures. *Virology* **1967**, *31*, 338–353.
30. Bolis, D.; Politou, A. S.; Kelly, G.; Pastore, A.; Temussi, P. A. Protein Stability in Nanocages: A Novel Approach for Influencing Protein Stability by Molecular Confinement. *J. Mol. Biol.* **2004**, *336*, 203–212.
31. Mahadevan, T. S.; Garofalini, S. H. Dissociative Chemisorption of Water onto Silica Surfaces and Formation of Hydronium Ions. *J. Phys. Chem. C* **2008**, *112*, 1507–1515.
32. Yang, J.; Meng, S.; Xu, L.; Wang, E. G. Water Adsorption on Hydroxylated Silica Surfaces Studied Using the Density Functional Theory. *Phys. Rev. B* **2005**, *71*, 035413.

33. Seder, R. A.; Hill, A. V. Vaccines against Intracellular Infections Requiring Cellular Immunity. *Nature* **2000**, *406*, 793–798.
34. Monney, L.; Sabatos, C. A.; Gaglia, J. L.; Ryu, A.; Waldner, H.; Chernova, T.; Manning, S.; Greenfield, E. A.; Coyle, A. J.; Sobel, R. A.; *et al.* Th1-Specific Cell Surface Protein Tim-3 Regulates Macrophage Activation and Severity of an Autoimmune Disease. *Nature* **2002**, *415*, 536–541.
35. Tang, F.; Li, L.; Chen, D. Mesoporous Silica Nanoparticles: Synthesis, Biocompatibility and Drug Delivery. *Adv. Mater.* **2012**, *24*, 1504–1534.
36. Wang, G.; Cao, R. Y.; Chen, R.; Mo, L.; Han, J. F.; Wang, X.; Xu, X.; Jiang, T.; Deng, Y. Q.; Lyu, K.; *et al.* Rational Design of Thermostable Vaccines by Engineered Peptide-Induced Virus Self-Biomineralization under Physiological Conditions. *Proc. Natl. Acad. Sci. U.S.A.* **2013**, *110*, 7619–7624.
37. Roser, B. Stable Liquid Vaccines and Drugs for the 21st Century. *Future Microbiol.* **2006**, *1*, 21–31.
38. Kaushik, J. K.; Bhat, R. Why Is Trehalose an Exceptional Protein Stabilizer? An Analysis of the Thermal Stability of Proteins in the Presence of the Compatible Osmolyte Trehalose. *J. Biol. Chem.* **2003**, *278*, 26458–26465.
39. Nassif, N.; Bouvet, O.; Noelle Rager, M.; Roux, C.; Coradin, T.; Livage, J. Living Bacteria in Silica Gels. *Nat. Mater.* **2002**, *1*, 42–44.
40. Baca, H. K.; Ashley, C.; Carnes, E.; Lopez, D.; Flemming, J.; Dunphy, D.; Singh, S.; Chen, Z.; Liu, N.; Fan, H.; *et al.* Cell-Directed Assembly of Lipid-Silica Nanostructures Providing Extended Cell Viability. *Science* **2006**, *313*, 337–341.
41. Chang, G. H.; Lin, L.; Luo, Y. J.; Cai, L. J.; Wu, X. Y.; Xu, H. M.; Zhu, Q. Y. Sequence Analysis of Six Enterovirus 71 Strains with Different Virulences in Humans. *Virus Res.* **2010**, *151*, 66–73.
42. Wang, G.; Li, X.; Mo, L.; Song, Z.; Chen, W.; Deng, Y.; Zhao, H.; Qin, E.; Qin, C.; Tang, R. Eggshell-Inspired Biomineralization Generates Vaccines That Do Not Require Refrigeration. *Angew. Chem., Int. Ed.* **2012**, *51*, 10576–10579.
43. Traggiai, E.; Becker, S.; Subbarao, K.; Kolesnikova, L.; Uematsu, Y.; Gismondo, M. R.; Murphy, B. R.; Rappuoli, R.; Lanzavecchia, A. An Efficient Method To Make Human Monoclonal Antibodies from Memory B Cells: Potent Neutralization of Sars Coronavirus. *Nat. Med.* **2004**, *10*, 871–875.